Digest Journal of Nanomaterials and Biostructures Vol. 6, No 4, October-December 2011, p. 1967-1981

STABILITY IN A NEURAL NETWORK-BASED NANO-TELEMANIPULATION THROUGH ADAPTIVE TUNING OF THE HAPTIC INTERFACE DISSIPATION

S. SAMADZADE[a*], M.H. KORAYEM[b], N.SARLI[c], M. ZAREINEJAD[c]
[a]*Department of Mechatronics, Islamic Azad University -Science and Research Branch,Tehran, Iran*
[b]*Robotic Research Laboratory, Center of Excellence in Experimental Solid Mechanics and Dynamics, School of Mechanical Engineering, Iran University of Science and Technology, Tehran, Iran*
[c]*New Technologies Research Center, Amirkabir University of Technology, Tehran, Iran*

A necessity for a reliable and accurate nano-telemanipulation system is to maintain stability during the process. The nano-environment is typically nonlinear and we cannot guarantee stability using criteria based on linear assumption. On the other hand, intermolecular forces dominant at nano scale render the nano-environment energy-producing. Numerous researches have attributed this to the substantial Van der Waals and capillary forces with respect to inertial forces in nanocosm. The purpose of this article is to propose a novel configuration for AFM-based nano-telemanipulation systems utilizing coupled stability and passivity theory which is extendable for any linear/nonlinear passive/active environment. The simulation results have shown that the three goals of stability, transparency and appropriate human perception are achieved. Specifically guaranteeing stability on the premise that some elements of the system are energy-producing is the main concern and treated by designing a suitable virtual coupling and haptic interface controller and by replacing the slave-side of the system with an appropriately trained neural network.

(Received October 12, 2011; accepted December 12, 2011)

Keywords: Telemanipulation, Stability, Passivity, Transparency, Virtual Environment, Neural Network, AFM

1. Introducation

Nano-manipulation is the precise mechanical interaction with nano-scale objects or environments. The nature of this interaction can be indentation, cutting, touching, pushing, pulling, or picking & placing nano-entities or nano-surfaces. In the past few decades attention to nano-manipulation has enormously grown. It is well understood that interactions among objects in the nanocosm are quite different from those in the macrocosm. To be more specific, surface forces and intermolecular forces (Van der Waals force) present at the nano-scale dominate gravitational and other more intuitive forces of the macro world with which human operators are usually familiar [1].

In this regard a large amount of research has been devoted to better understanding the nano-manipulation and identify the obstacles and develop effective solutions. One of the main challenges is that having visual feedback from the nano-world is not possible. On the other hand operations performed in nano-world produce positions and forces too small for the operator to

* Corresponding author: samadzade@gmail.com

feel hence introduction the position and force scaling factors that can instigate instability if not chosen appropriately. Furthermore nano-scale interactions involve complex nonlinear dynamics.

Nano-telemanipulation enables the operator to interact with the environment indirectly and "feel" reaction forces as if he/she is present in the environment. The prominent issue in this respect is to build a suitable interface between the nano-world and the macro-world which can handle all the issues mentioned above and even more hence a compensation for inaccessibility of the nano environment. Force feedback is important not only for enriching human operators' perception to indirectly feel interaction between an AFM probe tip and samples at the nano scale, but also for reliable telemanipulation of fragile, soft and complex nano objects such as biological samples or polymers [2].

From controls point of view, some principle aspects have to be taken into account since nano-telemanipulation involves feedback loops, i.e. human-master and environment-slave interaction, and controllers. Some of these issues are stability, transparency, and appropriate human perception. Stability means that the signals present in the system do not diverge. Transparency is a description of how similar the feeling of the operator from the environment through the teleoperator is to the actual feeling with no teleoperator in between. Comfortable human perception implies that humans may not really need to feel the exact environment impedance, rather a perception in a convenient impedance range is usually preferred for, in this way, they are able to accomplish the required task with more convenience. Undoubtedly this would sacrifice transparency partially.

Hollis used STM (Scanning Tunneling Microscope) as the nano-manipulator with a haptic device for teleoperated nanoscale topography [3]. Researchers have tried to integrate AFM with haptic techniques to assist nano-manipulation. For example in [4] and [5] a 1-DOF haptic device is constructed for feeling the vertical force acting on the AFM probe tip. However the force feedback technique used by them is very difficult to be implemented due to many unfamiliar forces and parameters in the nano-scale situation such as Van der Walls and capillary forces.

In [2] the nanoscale virtual coupling concept is introduced and the relation between performance, stability and scaling factors is explicitly derived. Due to a lack of visual feedback during AFM-based nano-manipulation, virtual reality with human machine interfaces for nano-telemanipulation were developed by some researchers [6-7].

In [7] the three main issues of stability, transparency and human perception are individually addressed and combined to achieve a stable system with adjusted forces for transparency and within the chosen impedance limits. Nano-environment active forces are considered in nano-telemanipulation design procedure for the first time and three approaches are reported. The implemented approach is to relax minimizing the energy constraints by supplying a maximum damping coefficient which would never be exceeded based on a passivity controller. Consequently active forces will be reduced but not removed and the Van der Waals interactions can still be felt by the operator.

The focus of this paper is to present a control configuration for an AFM-based nano-telemanipulation system with a virtual slave-side (i.e. virtual slave and environment). Considering the three main issues appropriately: stability, transparency and appropriate human perception. Our objective is that the human operator be able to fulfill the required task i.e. indentation of a surface with no trouble. For this the operator should be able to feel all the dominant forces present in the nanoworld distinctively. We introduce a novel nano-telemanipulation configuration based on passivity concept and a coupled stability analysis developed by Miller [8]. Miller's work is targeted for haptic systems. Since out work presents virtual-slave side teleoperation, we are granted permission to apply the results of his work.

To simplify the result of their work it can be said the energy producing component must be connected to another component that is capable of dissipating the excess energy if stability is to be achieved. This implies that the haptic device and virtual coupling must combine to provide dissipation and this further implicates that they must satisfy strict passivity conditions.

The article comprises four sections: in section two, the master and the slave robots are modeled and the effects of non-rigid AFM cantilever; in section three the stability of the designed

nano-telemanipulation system is analyzed section four concludes the article with simulation results and discussion.

2. Nano-Telemanipulation Syatem Modelling

2.1 Nano-telemanipulation system configuration

The proposed nano-telemanipulation system is depicted schematically in Figure 1. Operator exerts a force on the haptic device to perform an operation in nano-environment, the produced motion is transferred to slave robot (nano-piezo stage) through communication channels. The slave controller coordinates the position of the piezo-stage with that of the master's, the environment force is transferred back to the master side to be felt by the operator.

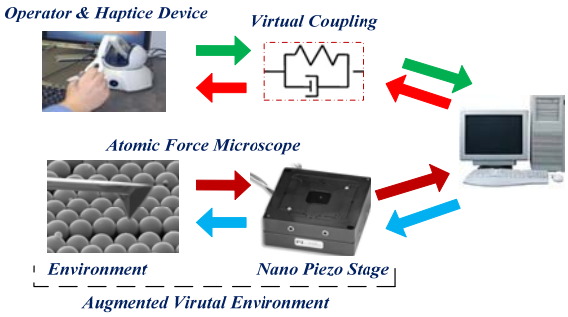

Fig. 1. Nano-Telemanipulation system

2.2 Master and slave robots

As the AFM tip approaches the sample surface the force $\mathbf{F_e}$ proportional to its distance from the surface (h) is applied on it. This force causes the probe deflection (ζ). The AFM tip as a single asperity contact tool is modeled using a mass-spring system as shown in Figure 2. The dynamics of the cantilever can be given as Eq.1.

$$m_c\ddot{\xi}+b_c\dot{\xi}+k_c\xi=-F_e \tag{1}$$

Where k_c, b_c, m_c, ξ, F_e are the cantilever stiffness and damping constant, mass, deflection and atomic interaction force respectively. The Derjaguin-Muller-Toporov model (DMT model) is suitable to describe the contact forces of hard, stiff materials with low adhesion forces and small tip radii. This model accounts for long-ranged attraction around the periphery of the contact area while the deformation geometry is Hertzian. According to this model, the normal interaction force can be described as

$$F_e=\begin{cases} -\dfrac{HR}{6h^2}-4\pi R\gamma_{SL} & h>a_0 \\ -\dfrac{HR}{6a_0^2}+\dfrac{4E^*\sqrt{R}}{3-3\nu_s^2}(a_0-z)^{3/2}h & h\le a_0 \end{cases} \tag{2}$$

a_0, E, ν, h, H, R,γ_{SL} are the intermolecular distance, the Young's modulus, Poisson's coefficient of the sample, the transient tip–sample separation, the Hamaker constant, the tip radius and the surface energy at solid-liquid interface respectively.

$h> a_0$ means noncontact region where Van der Waals force is assumed to be the only force in effect and the other condition is the contact region. In the noncontact region, the probe

approaches the sample or retracts from it while there is no contact between them. The attractive Van der Waals and the capillary force, and for the other, the summation of Van der Waals and repulsive contact force according to the DMT model are assumed. To better understand the nature of the aforementioned forces, a cantilever tip force is simulated while it is approaching a surface and is shown in Figure 3.
The slave dynamics (the piezo stage) can be given as:

$$\left(\frac{1}{(2\pi f_n)^2}\right)\ddot{x}_s+\left(\frac{1}{2\pi f_n Q}\right)\dot{x}_s+k_p x_s=\tau_s-F_e \tag{3}$$

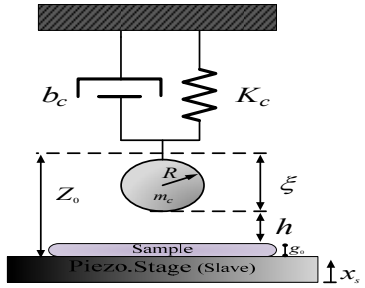

Fig. 2 Mass-spring model for the AFM probe

Where $w_n = 2\pi f_p$ is the resonance frequency, Q is the quality factor, x_s denotes the piezo-stage position, and τ_s is the salve control force. One goal of the nano-telemanipulation system is the coordination of the slave position and master scaled position. To achieve this, a simple proportional controller is adopted for the slave:

$$\tau_s=K(\alpha_p x_m-x_s) \tag{4}$$

in which K is the proportional gain and α_p is the position scaling factor. In this system, for proper interactions between the nano and the macro environments it is necessary to scale down/up the variables of position and force exchanged between the two worlds. The master dynamics is given by:

$$m_m\ddot{x}_m+b_m\dot{x}_m=\tau_m+F_h \tag{5}$$

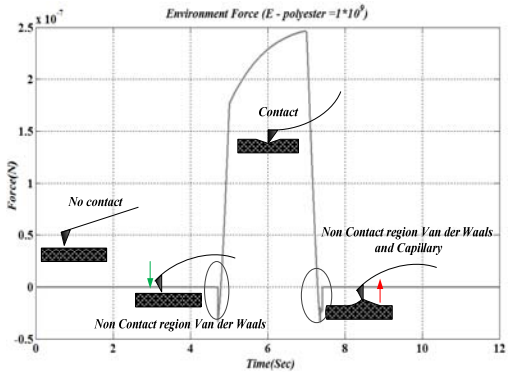

Fig. 3 Cantilever tip force while approaching a surface.

Where x_m denotes master position, m_m and b_m denote the inertia and viscous damping coefficient of the master, F_h denotes the force applied at the master side by the operator and τ_m is the master control signal.

2.3 The Environment force modification

The environment force has to be modified in three ways before it is reflected to the operator through τ_m:

1.Removing the effect of non-rigid AFM cantilever

Humans perceive the impedance of a surface (i.e. stiffness) by touching it by their hands. Therefore for a fine transparency no non-rigid object must exist between the operator and the surface being felt. The AFM Cantilever stiffness is definitely not infinite (thus non-rigid) and this matter should be treated properly. A simple solution as suggested in [7] is to mathematically manipulate the environment force to leave out the effect of the cantilever. As such, the reflected force would feel as though the cantilever is a rigid structure and the entire motion of the base is used to indent the substrate.

For example, consider a spring with stiffness K_s for surface and a spring with stiffness K_c for the contilever. The desired perception that we want the user to feel is a stiffness equal to K_s. However, the stiffness K_{eq} felt by human is the two springs in mechanical parallel, so:

$$F_t = \frac{K_s}{K_{eq}} F_e ; K_{eq} = \frac{K_s K_c}{K_s + K_c} \tag{6}$$

F_t is the transparent force, K_s is the surface stiffness, K_c is the probe stiffness, K_{eq} is the equivalent stiffness of the probe cantilever and the surface in paralled connection. Therefore, if the probe stiffness is increased $K_c \to \infty$, K_{eq} will approach K_s. Notice that the surface stiffness changes with variations of indentation depth. K_s could be approximated by its average value during indentation.

2. Surface Impedance Transformation:

At small scales, some materials may exhibit a very small stiffness. This might impede a clear distinction of the surface from noises inevitably present in the system or even from free motion (considering the existence of inherent damping in a haptic interface). On the other hand, a very hard surface may have a stiffness that is high from a human's aspect. The most straightforward approach to solve this issue is to linearly map the surface stiffness to a comfortable range for the human operator (Fig. 4). Taking the largest (k_e^{max}) and smallest (k_e^{min}) stiffness values encountered, and using two values as maximum and minimum stiffnesses (k_{max} and k_{min}) that are comfortable to work for the human we have:

$$F_{et} = \frac{k_{min} + (k_{max} - k_{min} / k_e^{max} - k_e^{min})(k_s - k_e^{min})}{K_{eq}} F_t \tag{7}$$

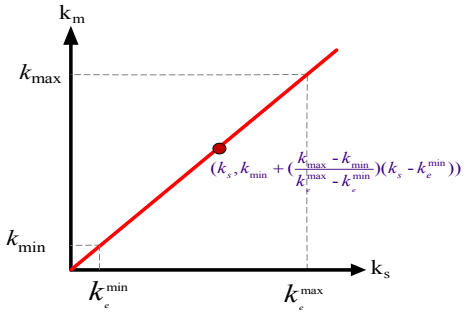

Fig. 4 Linear transformation from the surface stiffness to a comfortable range for the human operator

3. Force scaling:

Due to smallness, the previously modified force has to be magnified so that the operator can feel it.

Finally according to the above three modifications τ_m can be driven as:

$$\tau_m = \alpha_f F_{et} \tag{8}$$

3. Theories and definitions

To identify the individual components of a system in terms of energy dissipation or generation, passivity theory and to demonstrate stability of the overall nano-telemanipulation system coupled stability theory is used in this work.

3.1 Definition 1(continuous- time passivity):

A passive system is one for which the maximum amount of energy that can be extracted is equal to the initial stored energy plus the amount of energy input in the system. The continuous-time version of passivity states the following:

A system with input u and output y is passive if a non-negative function W (called a storage function) exists such that:

$$W(x(t)) \le W(x(0)) + \int_0^t y(\tau)u(\tau)d\tau - \rho\int_0^t y^2(\tau)d\tau - \varphi\int_0^t u^2(\tau)d\tau \tag{9}$$
$$\forall x \in R^n, x, t \ge 0$$

■

The Nyquist plot provides a convenient graphical method to determine passivity characteristics of linear systems. The frequency-domain interpretation is that the Nyquist plot lies in the closed right half plane (RHP).

3.2 Definition 2 (continuous- time Output Strictly passivity):

A system is output strictly passive (OSP), if Eq. 9 is satisfied with $\varphi=0$ and $\rho>0$, ρ is rate of energy dissipation. ■

The frequency-domain interpretation is that the Nyquist plot lies in a disk of radius $1/2\rho$.

3.3 Definition 3 (continuous- time Iuput Strictly passivity):

A system is input strictly passive (ISP), if Eq. 9 is satisfied with $\varphi>0$ and $\rho=0$, φ is rate of energy dissipation. ■

The frequency-domain interpretation is that the Nyquist plot lies to the right of the vertical line at φ in the RHP.

3.4 Definition 4 (Discrete- time passivity):

The discrete-time representation is obtained by replacing the integrals with summations:

$$W(x(k)) \le W(x(0)) + \sum_{k=0}^{i} y(k)u(k) - \rho\sum_{k=0}^{i} y^2(k) - \varphi\sum_{k=0}^{i} u^2(k) \tag{10}$$
$$\forall x \in R^n, x, k \ge 0$$

■

Storage function approach is particularly valuable in our study in that nonlinear virtual environment dynamics which cannot tractable by other methods; can be characterized using storage functions in as much as it views the system from its input/output only.

The circle criterion and a passivity result brought in [10] is used in this paper. These theories are brought for convenience.

3.5 Theorem 1[miller]:

If a system D that dissipates energy at a rate -δ (output strictly passive δ-OSP) is coupled to a system E that generates energy at a rate α (lack of α-ISP) less than δ, then the overall system is stable. For the coupled system to be output strictly passive,

$$\alpha < \delta \tag{11}$$

The proof of this claim is presented in appendix I.

3.6 Coupled stability based on energy consideration for nano-telemanipulation system

From an energy point of view, stability of a coupled system is preserved so long as there exists sufficient dissipation to dissipate any energy production. In this part the stability of the coupled system is studied based on the energy-based approach. If some parts of the system are energy-producing with a rate less than other components that are capable of dissipating the excess energy, the whole system will remain stable. This concept is explained based on the circle criterion [9].

According to the above concepts, the nano-telemanipulation system can be designed adhering to the rules below:

- The environment energy production rate can be defined by plotting the environment's energy (input output product).
- Calculating energy dissipation rate in the interconnected system of operator/haptic interface (by assuming a linear model for the operator, this value can be calculated based on appendix II [**lemma5**].
- Now if the produced energy in the environment is always less than δ or the relation α < δ always holds the system will remain stable (Fig.5).
- If the equation α < δ doesn't hold in some time intervals, stability can be guaranteed by injecting a damping into haptic device via the controller.

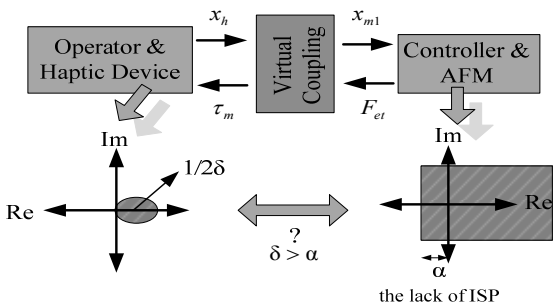

Fig. 5 Frequency domain interpretation of nano-telemanipulation system

The energy plot only gives us a visual perspective over environment circumstances and cannot represent the exact amount of produced energy. A mathematical formula is needed to find out this quantity. Miller proposed a relation for environment of the form $\psi(\chi,\nu,\eta)$ in which χ is input position and ν,η are its first and second derivatives respectively:

$$\alpha > \sigma \frac{T}{2} + \beta + \frac{2\phi}{T} \tag{12}$$

If the Eq.12 which is similar to Eq. 11 is established, the rate of produced energy will always remain less than its dissipation rate, ϕ،β ،σ are the representatives of stiffness, damping and inertia of the environment respectively (Figure 6).

The proof of this claim is presented in appendix II.

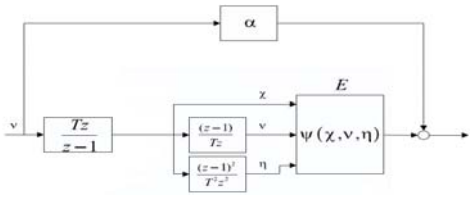

Fig. 6 Transformed environment block,α is an environment parameter measuring the lack of ISP

4. The proposed virtual nano-telemanipulation system

4.1 Virtual nano-telemanipulation system configurations

Figure 7 indicates a detailed schematic illustration of the proposed nano-telemanipulation system. The components of the system are: operator, haptic device, local controller, virtual coupling, augmented virtual environment (controller, slave robot (piezoelectric stage), AFM probe, and surface as the environment). As Miller et al in [9] show, the operator/haptic device must dissipate energy (satisfy continuous-time strict passivity) in order for the augmented virtual environment to produce energy.

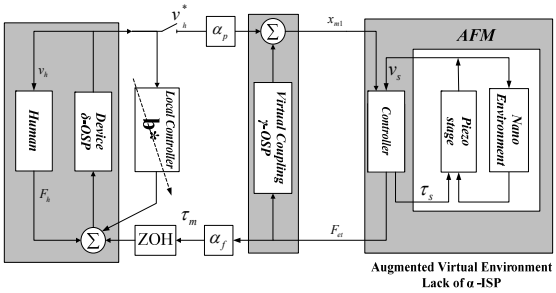

Fig. 7 The proposed nano-telemanipulation architecture

4.2 Neural-Based Nano-Telemanipulation System

To be able to apply the previous theorem, the scaling factors in Figure 7 are transmitted to the slave-side with a simple loop transformation, and because the dynamics of the environment under study (Eq.13) is not included in the Miller's classifications of environments, then it is proposed to train a neural network to emulate the augmented virtual environment behavior. The augmented virtual environment dynamic is:

$$\left.\begin{aligned} &x_{m1}=u, F_e=y\\ &x_1=x_s\\ &x_2=\dot{x}_1=\dot{x}_s\\ &x_3=\xi\\ &x_4=\dot{x}_3=\dot{\xi} \end{aligned}\right\} \Rightarrow \begin{cases} h>a_0\\ \dot{x}_4=\dfrac{HR}{6h^2}-k_c x_3-b_c x_4\\ h\le a_0\\ \dot{x}_4=-\underbrace{\left(-\dfrac{HR}{6a_0^{\,2}}+\dfrac{4E^*\sqrt{R}}{3-3\nu_s^2}\left(a_0-z-z_c\right)^{3/2}h\right)}_{F_e}-k_c x_3-b_c x_4 \end{cases} \tag{13}$$

$$\Rightarrow y=(k_p+k_s)x_1+b_s x_2+\dot{x}_2-k_p u$$

Substituting it with the trained neural network, the final transformed system is illustrated in Figure 8.

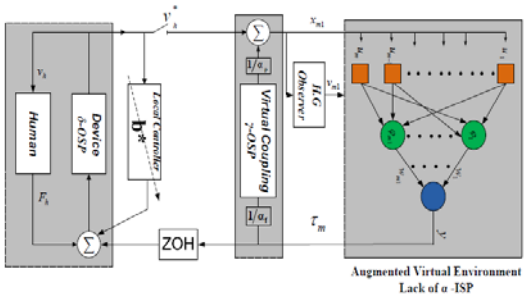

Fig. 8 The neural-based Nano-telemanipulation architecture after loop

The following parameters are introduced as instantaneous representatives of the neural-based augmented virtual environment:

$$\begin{cases} \sigma = \dfrac{\psi(b,0) - \psi(a,0)}{a-b}, (a \neq b) \\ \beta = \dfrac{\psi(x_{m1},0) - \psi(x_{m1},v_{m1})}{v_{m1}}, (v_{m1} \neq 0) \end{cases} \tag{14}$$

where $\tau_m = \psi(x_{m1}, v_{m1})$ is the neural-based augmented virtual environment function. Now the condition that guarantees passivity according to (section 3.1) is:

$$\alpha \geq \frac{1}{2}\sigma T + \beta \tag{15}$$

4.2.1 Neural Network specification

To produce acceptable outputs, it is required that the neural network be trained appropriately. Therefore we have to supply the neural network with more as well as richer data. In that regard the original nano-telemanipulation system was tested by an operator.

The utilized networks could be adapted if there is any changes in environment, this network is implanted using the MATLAB neural networks tool box and trained with *Levenberg-Marquardt* method.

In order to obtain training data the differential model of the environment was put in the hardware loop and 30 inputs- outputs were registered with their derivatives so the effect of speed is also considered, this method may increase the noise levels and could be replaced with an observer. Two networks were arranged, one with position inputs and second with position and velocity input.

4.2.2 Virtual Coupling

Virtual coupling is simply a spring and a damper in parallel connection and its role is to help guarantee stable interaction without drastically influencing the perception of the environment and it has to satisfy a certain OSP condition (refer to Appendix I). It is desirable to eliminate the virtual coupling because it is detrimental to the real perception of the operator from the environment. Unfortunately, when it is removed stability margins decline dramatically. To achieve a virtual coupling with a minimum effect on perception its damping is set to zero and the stiffness is chosen as: $K = 2\delta/T$.

4.2.3 Local controller

Recall that α is amount of excess passivity in the operator/device block and has units of damping. It is important to note that α is a tool; including it in the environment analysis provides

us with insight on how the overall system will behave once the operator/device block and the augmented virtual environment are connected. Eq.11 can be used to determine the amount of physical damping (δ) required in the device.

Having calculated the required damping in the device for a stable interaction it is quite possible that the inherent damping of the haptic interface not be adequate (as already mentioned). In this case the solution is to inject the required damping b^* through a (simple feedback) local controller as shown in Figure 8 on the right side of the device block.

4.2.4 Human Operator

Concerning the operator, it is assumed that he/she is supplying passive excitation. In fact the human operator is even capable of playing a stabilizing role in the closed-loop system.

4.2.5 Summary

A Summary of the proposed procedure for designing a virtual-slave–side nano-telemanipulation system is shown in the following:

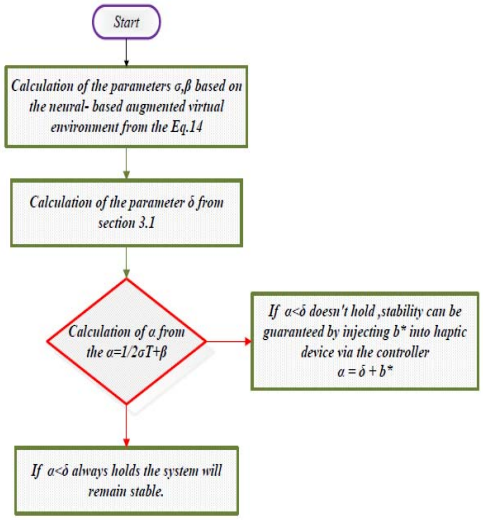

Fig. 9 Guaranteed stability algorithm in the neural-based nano-telemanipulation

5. Results and discussion

To derive speed from position data produced from encoder the simplest way is differentiation. However, differentiation introduces too much noise for the neural network to learn the true velocity behavior. Therefore a high-gain observer was used to produce velocity. Figure 9 represents both methods to derive velocity. This figure shows velocity is approximated smoothly with small deviations from differentiated position.

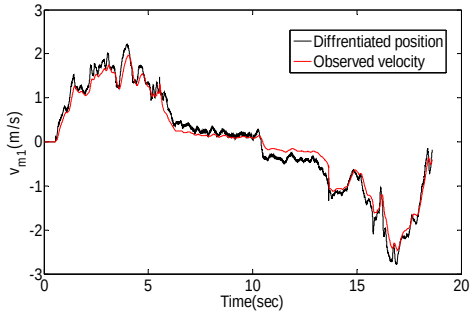

Fig. 10 Velocity obtained from two methods (differentiating and observing)

We are performed on two different environment with Young modulus E=1e^6 and E=10e^6, and υ=0.2

In every experiment indentation depth or operation speed (slave speed) was changed so that variegated inputs would be provided 30 experiments were run all in all. The fixed parameters in the experiments were chosen as follows:

$$m_c = 4.5\times10^{-11}, b_c = 1.4\times10^{3}, k_c = 40, f_p = 450, Q = 20, k_p = 1, H = 10^{-19}, R = 20\times10^{-9}, a_0 = 1A^0, v = 0.2, g_0 = 10nm,$$
$$k_{\max} = 200, k_{\min} = 40, k_e^{\min} = 2\times10^{-3}, k_e^{\max} = 2\times10^{3}, K = 150, \alpha_p = 0.6\times10^{-6}, \alpha_f = 6\times10^{6}$$

Since K_s varies with variation of indentation depth, it is approximated as its value when the penetration depth is 2.5 nm. The augmented virtual environment and the virtual coupling updating rate is 1000 Hz. α_p is chosen according to the master and slave motion ranges. To get a good compromise between easiness and accuracy of manipulation, the value $\alpha_p = 0.6\times10^{-6}$ is selected (the master motion range corresponds then to a displacement of 50μm for the slave) and α_f is selected so that the system remains stable

Figures 10 - 13 depict the results of an experiment on a virtual sample with $E = 10GPa, \upsilon = 0.2$. In Figure 10 master and slave positions are shown. Position drift is spotted when the slave is in contact with the environment where free motion is performed with perfect coordination. Figure 11 illustrates the tip-surface distance in the same experiment. In this graph negative values denote penetration depth in the sample. The maximum indentation depth is nearly 2.7 nm.

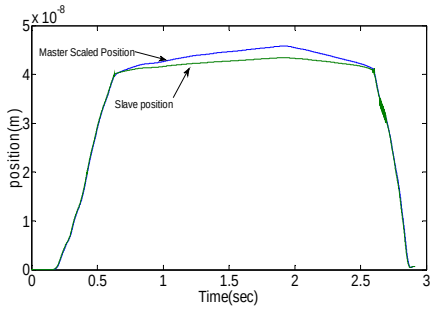

Fig. 11 Master and slave position in an indentation task on a virtual sample with $E = 10GPa, \upsilon = 0.2$

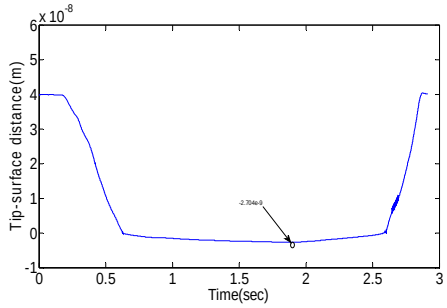

Fig. 12 Tip-surface distance in an indentation task on a virtual sample with $E = 10GPa, \upsilon = 0.2$

Figure 12 shows the reflected force to the operator. The initial small positive peak (within 0.62-0.65) is attributed to the Van der Waals force, the next large negative peak (within 0.65-2.57) is pertaining to the contact force and the last small negative peak (within 2.57-2.62) is pertinent to the adhesion force.

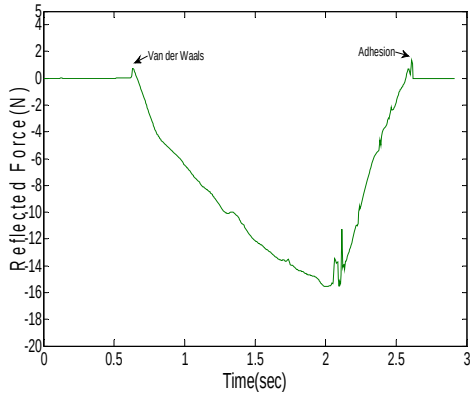

Fig. 13 Reflected force to the operator in an indentation task on a virtual sample with $E = 10GPa, \upsilon = 0.2$

In Figure 13 adaptive damping coefficients implemented on the master to stabilize the system in the experiment are plotted. Zero values imply the system's own dissipation including inherent master and human damping is sufficient to stabilize the system. In other cases necessary damping is applied and the system always remains stable. Finally, the three figures are the same task with a harder material ($E=1e^6$).

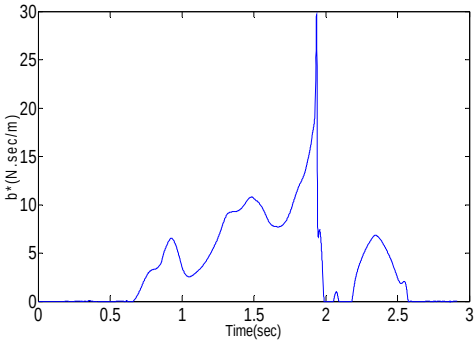

Fig. 14 Adaptive damping implemented on the master manipulator in an indentation task on a virtual sample with $E = 10GPa, \upsilon = 0.2$

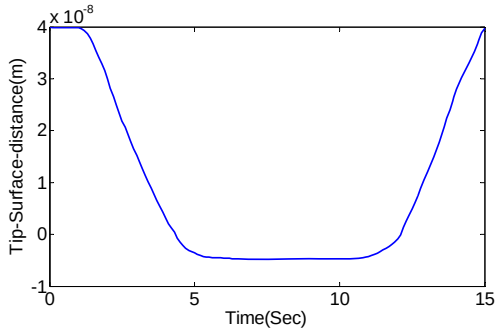

Fig. 15 Tip-surface distance in an indentation task on a virtual sample with $E = 1GPa, \upsilon = 0.2$

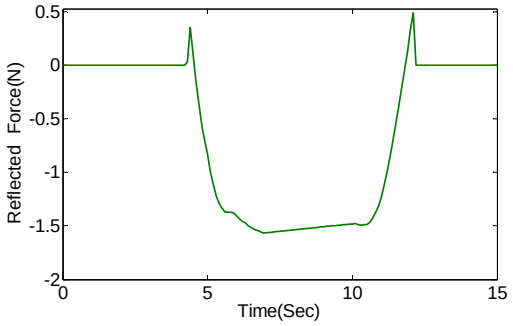

Fig. 16 Reflected force to the operator in an indentation task on a virtual sample with $E = 1GPa, \upsilon = 0.2$

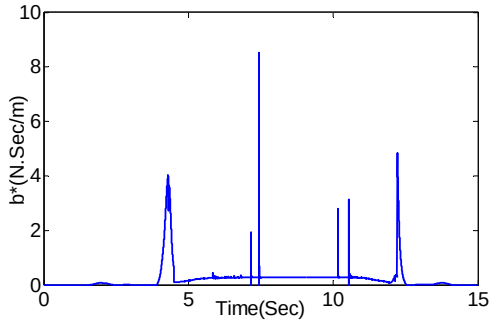

Fig. 17 Adaptive damping implemented on the master manipulator in an indentation task on a virtual sample with $E = 1GPa, \upsilon = 0.2$

6. Conclusion

A novel approach for designing a nano-telemanipulation system is proposed which can guarantee a stable interaction with nonlinear and inherently active nano virtual environments. The method relies only on the haptic interface damping (either inherent or through a damping injection controller) to stabilize the nano-telemanipulation system.

The proposed approach is applicable to other 1-DOF tasks in virtual environments. Here is how it can be achieved: the operator performs the task in the original virtual environment to provide the respective neural network with necessary data for training. After the training procedure the main augmented virtual environment block is replaced with the generated neural network. Afterwards the block responsible for calculation and implementation of the adaptive damping to the master controller is added to the simulation. Now the operator is ready to execute his task stably with no extra dissipation due to blind damping injection.

References

[1] M. Sitti, and H. Hashimoto, IEEE/ASME Trans. on Mechatronics, **8**(2), 287 (2003).
[2] S. G. Kim and M. Sitti, IEEE Transactions on Automation. Science and Engineering, **3(**3), 240 (2006).
[3] M R.L. Hollis, S. Salcudean, and D. W. Abraham, Proc. IEEE Int. Conf. Micro Electro Mechanical Systems, pp. 115-119,(1990).
[4] M. Sitti and H. Hashimoto, Proc. IEEE Int. Conf. Intelligent Robots and Systems, pp:1739–1746,(1998).
[5] M. Guthold, M. R. Falvo, W. G. Matthews, S. washburn, S. Paulson, D. A. Erie, IEEE/ASME Transactions on Mechatronics **5**(2), 189 (2000).
[6] R. Falvo, R. Superfine, S. Washburn, M. Finch, R. M. Taylor II, V. Chi and Jr. F. P. Brooks, Proc. of the Int. Symp. Science and Technology of Atomically Engineered Materials, Richmond,pp. 579-586,(1995).
[7] C. D. Onal, C. Pawashe, and M. Sitti, "A scaled bilateral control system for experimental 1-D teleoperated nanomanipulation applications," IEEE/RSJ International Conference on Intelligent Robots and Systems San Diego,CA,USA,(2007).
[8] B.E. Miller, J.E. Colgate and R.A. Freeman, "Guaranteed Stability of Haptic Systems with Nonlinear Environments," IEEE Transactions on Robotics and Automation, Vol.16, No.6,(2000).
[9] B.E. Miller, J.E. Colgate and R.A. Freeman, "Passive Implementation for a Class of static Nonlinear Environments in Haptic Display," IEEE International Conference on Robotics and Automation, Detroit, MI, IEEE, 4, pp. 2937-2942,(1999).
[10] H.K Khalil, Nonlinear Systems: Second Edition, Prentice Hall Inc., New Jersey.

Appendix I

The proof for Eq.11 is brought in [9] completely. The parallel connection of the transformed blocks D (δ-OSP) and V.C. (γ-OSP) is analogous to resistors in parallel, producing a block that is $\delta\gamma/\delta+\gamma$–OSP. Consider a storage function W_1, for the parallel connection of D and V.C. Since this connection is $\delta\gamma/\delta+\gamma$–OSP the incremental version (change in energy over a time-step) of the storage function can be expressed as Eq.14 and consider a storage function W_2, for the transformed augmented virtual environment block that exhibits a lack of OSP of an amount α, therefore Eq.15. For $\delta,\gamma > 0$ it follows Eq.16:

$$W_1 \le -FV-\frac{\delta\gamma}{\delta+\gamma}V^2 \tag{15}$$

$$W_2 \le FV+\alpha V^2 \tag{16}$$

$$W_I=W_1+W_2 \Rightarrow \Delta W_I \le \left(\alpha-\frac{\delta\gamma}{\delta+\gamma}\right)V^2 \tag{17}$$

Therefore, $\alpha < \delta\gamma/\delta+\gamma$ and this immediately follows: $\alpha < \delta$

The above result implies that for stability the rate energy is produced by the augmented virtual environment must remain less than the rate of dissipation by the device.

Appendix II

This appendix will summarize interconnection theories for passivity. The following Lemmas summarize the interconnection between two dissipative blocks, A1 and A2 with storage functions U1 and U2 respectively (Fig. 18).

Lemma 5. Let A1 be δ_1-dissipative and A2 be δ_2-dissipative with $\delta_1 + \delta_2 > 0$. The parallel connection of systems is δ-dissipative: $\delta = \delta_1\delta_2 / \delta_1 + \delta_2$. A valid storage function is : U= U1+ U2.

Lemma 6 . Let A1 be δ_1-dissipative and A2 be δ_2-dissipative with $\delta_1 + \delta_2 > 0$. The feedback connection of systems is δ-dissipative: $\delta \leq \delta_1 + \delta_2$. A valid storage function for is : U= U1+ U2.

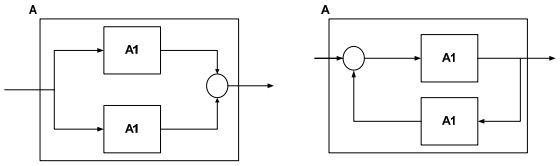

Fig. 18 On the left, dissipative blocks A1 and A2 in parallel defining A. On the right, dissipative blocks A1 and A2 in feedback defining A.